The Visual Computer
This is a post-peer-review, pre-copyedit version of an article published in The Visual Computer. The final authenticated version is available online at: https://doi.org/10.1007/s00371-018-1486-x.

Visual Analysis of Retinal Changes with Optical Coherence Tomography

Martin Röhlig · Christoph Schmidt · Ruby Kala Prakasam · Paul Rosenthal · Heidrun Schumann · Oliver Stachs

Accepted: 24. January 2018 / Online date: 20. February 2018

Abstract Optical coherence tomography (OCT) enables noninvasive high-resolution 3D imaging of the human retina, and thus plays a fundamental role in detecting a wide range of ocular diseases. Despite the diagnostic value of OCT, managing and analyzing resulting data is challenging. We apply two visual analysis strategies for supporting retinal assessment in practice. First, we provide an interface for unifying and structuring data from different sources into a common basis. Fusing that basis with medical records and augmenting it with analytically derived information facilitates thorough investigations. Second, we present a tailored visual analysis tool for presenting, emphasizing, selecting, and comparing different aspects of the attributed data. This enables free exploration, reducing the data to relevant subsets, and focusing on details. By applying both strategies, we effectively enhance the management and the analysis of retinal OCT data for assisting medical diagnoses. Domain experts applied our solution successfully to study early retinal changes in patients suffering from type 1 diabetes mellitus.

Keywords Visual analysis · Optical coherence tomography · OCT data · Ophthalmology · Retina

This work has been supported by the German Research Foundation (project VIES) and by the German Federal Ministry of Education and Research (project TOPOs).

Martin Röhlig
Institute for Computer Science, University of Rostock, Rostock, Germany
E-mail: martin.roehlig@uni-rostock.de

Christoph Schmidt
Institute for Computer Science, University of Rostock, Rostock, Germany
E-mail: christoph.schmidt2@uni-rostock.de

Ruby Kala Prakasam
Department of Ophthalmology, University of Rostock, Rostock, Germany
E-mail: rubykala.prakasam@med.uni-rostock.de

Paul Rosenthal
Institute for Computer Science, University of Rostock, Rostock, Germany
E-mail: research@paul-rosenthal.de

Heidrun Schumann
Institute for Computer Science, University of Rostock, Rostock, Germany
E-mail: heidrun.schumann@uni-rostock.de

Oliver Stachs
Department of Ophthalmology, University of Rostock, Rostock, Germany
E-mail: oliver.stachs@uni-rostock.de

1 Introduction

In the context of ophthalmology, optical coherence tomography (OCT) is a widely applied method to support the medical diagnosis of various ocular diseases. Based on high-resolution 3D imaging of the human retina, many medical conditions can be detected. Examples are diabetic retinopathy, age-related macular degeneration, and glaucoma induced retinal changes [41]. The diagnostic procedures involve searching for subtle retinal changes, analyzing multiple OCT datasets, and correlating findings with other clinical information. Especially for identifying early signs or investigating progressions, all of these steps are mandatory. Yet, due to the complexity of the data, already exploring a single volumetric OCT dataset can be difficult. This becomes even more complicated if details in multiple datasets have to be compared or different proprietary data formats have to be dealt with, e.g., in case of datasets from different OCT devices. Hence, managing and analyzing OCT data and relating them to other information are challenging and time-consuming tasks.

We present an interactive visual approach to address the peculiarities of OCT data: (i) data originating from different acquisition modalities and (ii) volumetric data of high spatial resolution combined with extracted information. Our contributions are:

Unified Data Management: We convert and structure OCT data from different sources into a common basis, enabling unified data access and management. We fuse that basis with other medical records and augment it with analytically derived information.

Interactive Visual Analysis: We propose a novel visual design for presenting, emphasizing, and comparing different aspects of the data. Coordinated interaction facilitates exploration, selecting relevant subsets, and inspecting details on demand.

This paper covers an extended version of our initial work on visual analysis of OCT data [34]. Here, we introduce a new compact representation of multiple OCT datasets that enables visual comparison and eases the identification of subtle retinal changes. We integrate the visualization, interaction, and computation techniques in a visual analysis workflow and describe how it helps to tackle the problem at hand. As another extension, we outline our collaboration with medical experts, which allowed us to understand their current analysis procedure, define design requirements, and test our solutions. The combined work steered the development and helped to address the experts' needs. Lastly, we broaden the discussion of our results, point out limitations, and indicate future research directions.

The remainder of the paper is structured as follows. The background and current analysis procedure are described in Section 2. Related work is reviewed in Section 3 and design requirements are listed in Section 4. The unified data management and the interactive visualization are detailed in Sections 5 and 6. In Sections 7 and 8, application results and user feedback are presented. Finally, limitations and future work are discussed in Section 9.

2 Background

The structure of the multi-layered retina in the posterior segment of the eye cannot be examined with conventional ophthalmic methods. Starting with ultrahigh-resolution OCT-based retinal imaging [10], it is now possible to display different layers of the retina and provide unmatched detail and contrast images in an extraordinary way. This improves the diagnosis of pathologies, even at an early stage.

2.1 Optical Coherence Tomography Data

State-of-the-art OCT devices are based on frequency domain optical coherence technology (also referred to as swept source OCT or spectral domain OCT). The OCT procedure is noninvasive and completely safe without light hazard. A laser beam scans the retina using dedicated scanning patterns in combination with active eye tracking. In this process, consecutive 1D reflectivity profiles (A-scans) are acquired. The profiles contain information about the spatial dimensions and location of inner structures. Cross-sectional 2D image slices (B-scans) are obtained by laterally combining a series of these axial depth scans (A-scans). Multiple 2D image slices are then merged into a 3D tomogram. Commercially available systems currently have an approximate axial and lateral resolution of $3-7\,\mu m$/pixel and $5-10\,\mu m$/pixel respectively, covering an area of about 9×9 mm at 2 mm scan depth. The actual image resolution depends on acquisition settings and differs between manufacturers. As an example, datasets from the Spectralis OCT (Heidelberg Engineering GmbH) can have a maximal resolution of 1536 equally spaced B-scans with 1536×512 pixels.

The raw volumetric image data are further processed using various image analysis techniques, including image registration and noise reduction [3]. Complementary segmentation algorithms are applied on the datasets to extract up to 11 retinal layers [13]. Optionally, measurements are computed to additionally characterize the data, e.g., thickness maps of the layers. Figure 1 illustrates common components of OCT data. Altogether, a typical OCT dataset contains one 3D tomogram composed of multiple 2D image slices, several extracted layers, and various computed measurements. In addition, one fundus image of the interior surface of the eye around the OCT acquisition area is usually recorded, e.g., via scanning laser ophthalmoscopy.

2.2 Current Analysis Procedure

Given the complexity of OCT data, it is challenging to identify subtle and localized changes of various abnormal conditions of the retina. Currently common analysis procedures involve both analyzing individual datasets and comparing multiple datasets.

Individual OCT datasets are analyzed in search for retinal changes related to signs, symptoms, and other clinical information of ocular diseases. This is usually done to diagnose subtle variations that cannot be captured with other examination methods or to obtain additional findings for investigating indications of a disease.

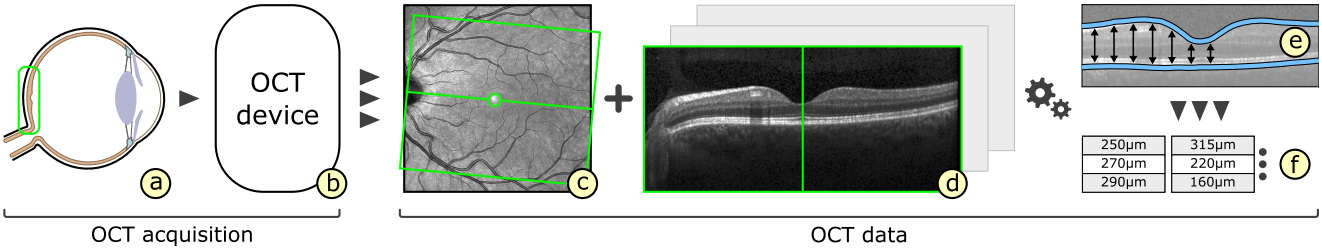

Fig. 1. Common data components of volumetric OCT datasets. During acquisition, primarily the area around the macula and the optic disk (a) are captured with an OCT device (b). The resulting data consists of a fundus image of the interior surface of the eye (c) and multiple 2D image slices that form a 3D tomogram (d). Further processing allows to extract several retinal layers (e) and computed measurements (f), e.g., the layer thickness.

To detect localized retinal changes, the ophthalmologists have to explore three main aspects of OCT data: the raw tomogram, the extracted layers, and associated measurements. This can entail high manual effort. For example, the experts are often required to inspect individual image slices or extracted layers one by one. This causes strain, particularly in case of high-resolution datasets that comprise hundreds of image slices. However, a high density of image slices is necessary for an exact assessment of certain retinal areas, e.g., to detect small macular holes [5] and to reduce errors of computed measurements [30].

Alternatively, current analysis procedures are either based on selective measurements or on excessive global data reduction with regard to both, space and information. In the first case, measurements are computed for specific points in the data. Depending on the analysis goal, the data are sampled at a known location, e.g., where changes are visible in the fundus image. As another example, several sample points may be aligned to form custom sample patterns, e.g., to obtain approximate layer profiles from the center of the fovea in a certain direction. In the second case, the tomogram or the extracted layers are subdivided into coarse sectors and for each sector aggregated measurements are retrieved. The locations and areas of these sectors are, for example, defined according to grids from the Early Treatment Diabetic Retinopathy Study (ETDRS) [12]. These grids consist of nine regions that subdivide central, pericentral, and peripheral concentric rings around the fovea in nasal, temporal, inferior, and superior direction. As a result, entire OCT datasets are represented by few values. While this reduces the amount of information that has to be examined, it also renders the analysis results spatially unspecific.

Multiple OCT datasets are analyzed to compare selected datasets either with each other, e.g., a baseline to a follow-up dataset, or to reference data, e.g., datasets of patients to data of a control group. Such analyses are more involved and go beyond the steps necessary for analyzing individual datasets.

In the first case, ophthalmologists typically have to open separate views for each dataset. The views are then individually adjusted to keep them consistent and to ensure that matching parts per dataset are shown. Searching for differences is realized by juxtaposing the views or by switching back and forth between them. Yet, manually coordinating and inspecting the separate views is perceived cumbersome.

In the second case, ophthalmologists have to rely on data reduction, e.g., based on ETDRS grids as described above. To start, aggregated measurements for all considered datasets are computed. These values are then exported for further statistical analysis. Yet, the available export functionality is usually limited and so, dozens of values per dataset have to be copied by hand from the acquisition platform to the analysis software. Particularly in case of larger studies with hundreds of OCT datasets, this is time-consuming and error-prone. Moreover, the statistical outcome often only shows comparisons of mean values from larger areas, e.g., sectors of ETDRS grids. However, it does not disclose subtle local variations or the actual morphological changes.

In addition to analyzing OCT datasets, ophthalmologists have to relate their findings to other clinical data, e.g., information on data quality, patient-related records, and results of other examination methods. For this purpose, they typically have to rely on third-party software to show necessary information on demand. This further complicates the data analysis.

Our new interactive visual approach shows such information directly and simplifies identifying and processing abnormal retinal characteristics.

3 Related Work

Current analysis procedures are based on a combination of commercial and non-commercial OCT software and

general-purpose analysis software. Besides visualizing OCT data, statistical evaluation of pointwise measurements or aggregated values of certain regions is a common approach in ophthalmic research. Particularly, the thickness of retinal layers has been continuously used as a basis for investigations of early structural changes of the retina for a variety of diseases, e.g., diabetes mellitus [7, 9, 14] or glaucoma [6]. The statistical results are reported via basic displays, e.g., tables, box-plots, or color-coded ETDRS grid diagrams. Commercial and non-commercial software offer additional methods for visually analyzing OCT data.

3.1 Commercial Analysis Software

Commercial OCT software is predominantly distributed by OCT device manufactures. Currently, several major platforms are available, including software from Nidek, Optovue, Zeiss, Topcon, Heidelberg Engineering and others. Modern 3D retinal imaging has led to advances regarding the display and analysis functionality [28, 40]. Yet, commercial software typically matches the respective device's capabilities and hence, software features often differ between tools. In general, they all support managing, analyzing, and presenting OCT data.

For managing OCT data, users have to rely on device-specific file formats and databases. This prohibits the exchange of OCT data. Moreover, it complicates analyzing and comparing datasets from diverse manufactures, e.g., due to deviations in resolution, numerical precision, registration, noise reduction, and image segmentation [5].

For analyzing OCT data, users take measurements based on OCT tomograms directly or based on prior extracted retinal layers. Yet, supporting algorithms and associated parameters are proprietary, and thus deviations between measurements may occur [35]. This makes comparisons of analysis results from different tools error-prone. Moreover, while some tools allow to relate measurements to a proprietary normative database, available methods generally do not support comparative analysis of data from different individuals or groups. Thus, such investigations have to be conducted based on exported data and external software.

For displaying OCT data, three types of presentations are common. First, the acquired 2D image slices are shown individually. This allows to view details but flipping through the images is time-consuming. Second, a fundus image is shown together with superimposed retinal layers. This helps to link the layers to the fundus but the layers can only be examined one at a time. Third, the OCT tomogram is shown in 3D. This provides an overview of the data but adjusting the visual representation, e.g., via navigation, is often limited. Also, combined 3D visualizations of the tomogram and the layers are typically not available, and thus spatial relationships might go unnoticed. Other drawbacks include inappropriate hard-wired color-coding, lacking consideration of data quality, and limited support for additional information.

Given those limitations, ophthalmologists are currently advised to use the same OCT device and associated analysis software for all examinations of their patients to ensure comparability of results [5].

3.2 Non-Commercial Analysis Software

Besides commercial software, few approaches for visually analyzing retinal OCT data exist. The open-source software ImageJ can be used to analyze OCT images [37]. The Iowa Reference Algorithms are a research-oriented software that supports segmentation, visualization, and measurement of retinal layers [17]. Instead of extracted retinal layers, reflectivity profiles allow to characterize retinal conditions [16]. 3D visualization based on ray-tracing and artificial shadows shows subtle structures more distinctly but images can take multiple seconds to render [20]. Likewise, virtual reality can be employed to enhance spatial perception and facilitate an immersive data access [1, 38]. However, selecting and comparing parts of multiple datasets or relating them to other information is often not considered. Real-time 3D rendering has also been studied to enable online display of OCT tomograms during acquisition and to preselect relevant subsets for reduced storage costs [32, 39]. Yet, in-depth analysis of details still has to be done in a post-acquisition stage.

Aside from ophthalmology, visual analysis of optical coherence tomography data is an inherent part of other fields as well. Examples include different biomedical applications, e.g., OCT-based exploration of cerebral vessel walls [18], or material science, e.g., detection of subsurface defect [11] or investigation of internal structures of bast fibers [31]. Although visual analysis proved to be useful in those domains, respective solutions are not directly applicable to retinal OCT data.

In summary, existing works offer different approaches for managing, analyzing, and presenting OCT data. Yet, each solution covers only a certain aspect. Our goal is to develop an integrated approach that (i) incorporates previous efforts regarding a common data basis, (ii) extends that basis with supplementary information, (iii) visualizes and emphasizes different aspects of the attributed data, and (iv) allows selecting and comparing relevant subsets. With the resulting flexibility, we are able to address the peculiarities of OCT data and support the retinal assessment.

4 Requirements

Discussing with domain experts and analyzing existing approaches, we derived two lists of requirements related to: (i) managing OCT data and (ii) visualizing OCT data.

Data-related Requirements: The data-related requirements reflect the experts' needs with regard to managing and processing OCT data. We derived the following list by talking with the experts about current limitations and by analyzing the computation and storage capabilities of OCT devices.

Manage data from different manufacturers (DR_1): The experts require support for OCT data from different manufacturers. Particularly, they ask for a unified access for datasets acquired using different OCT devices. So, providing a common data basis that incorporates all main aspects of OCT data, i.e., the raw tomogram, extracted retinal layers, and computed measurements, is a fundamental requirement.

Common and open data format (DR_2): Based on the common data basis, the experts want to make the data openly available. This is to allow easy exchange, storage, and further processing of datasets. Hence, the second requirement is to provide a common and open data format.

Derive and incorporate additional information (DR_3): Directly incorporating and retrieving additional information is another request from the experts. This is to provide them with further details to help to characterize the condition of the retina. Especially, measurements based on extracted layers are necessary, as they allow to capture subtle changes which would be hard to identify by looking at the raw OCT data alone. Therefore, augmenting OCT datasets with respective information has to be supported.

Coherent analysis pipeline (DR_4): Altogether, the experts wish for a consistent set of data processing and computation methods. This is to ensure comparability of analysis results across datasets. These results also have to be reflected in the common data basis. Accordingly, the attributed data should provide a starting point for a coherent analysis and visualization pipeline.

Visualization-related Requirements: The visualization-related requirements correspond to the experts' goals when visually analyzing OCT data. We derived the requirements following a participatory design process. Together with the experts we made general design decisions and devised suitable visualization concepts:

Explore and relate different data aspects (VR_1): To detect localized retinal changes, the experts have to explore the raw tomogram, the extracted retinal layers, and computed measurements. In this regard, established display concepts have to be considered (cf. 3.1). At the same time, the context of the three data aspects has to be maintained. Therefore, visualizing the aspects and interactively relating them needs to be facilitated.

Show related information on demand (VR_2): For assessing the condition of the retina, the experts have to relate findings to other information. So, besides incorporating supplementary information in the common data basis (cf. DR_3), showing that information on demand together with the OCT data is required.

Discover and inspect regions of interest (VR_3): The experts want to have quick access to different parts of the data and to be able to inspect these parts in greater detail. This is particularly important in case of high-resolution datasets and subtle retinal changes. Hence, identifying, highlighting, and selecting regions of interest is another basic requirement.

Compare multiple datasets (VR_4): The experts need to compare findings in multiple OCT datasets. This involves both comparing individual datasets to each other and analyzing datasets in relation to reference data. Thus, we consider visually comparing multiple datasets as a necessary design requirement.

Based on the experts' demands, we incorporate a unified data management that addresses requirements $DR_1, ..., DR_4$ and develop an associated visualization tool to meet requirements $VR_1, ..., VR_4$.

5 Unify, Structure & Enhance Data

Currently, no standardized description of OCT data exists. This hinders data processing and analysis. Moreover, the raw data alone may not provide enough information for definite diagnoses. In an initial effort to address these issues, we integrate a common data basis and enrich that basis with derived layer attributes.

5.1 Common Data Basis

No matter if clinical or research use is intended, it is often beneficial or at times even needed to take data from different OCT devices into consideration. The most problematic part with this is the fact that manufacturers only provide software for the data of their own OCT scanners. Consequently, there is no approved way of viewing, analyzing, or comparing data from different devices. Furthermore, there are only limited possibilities to

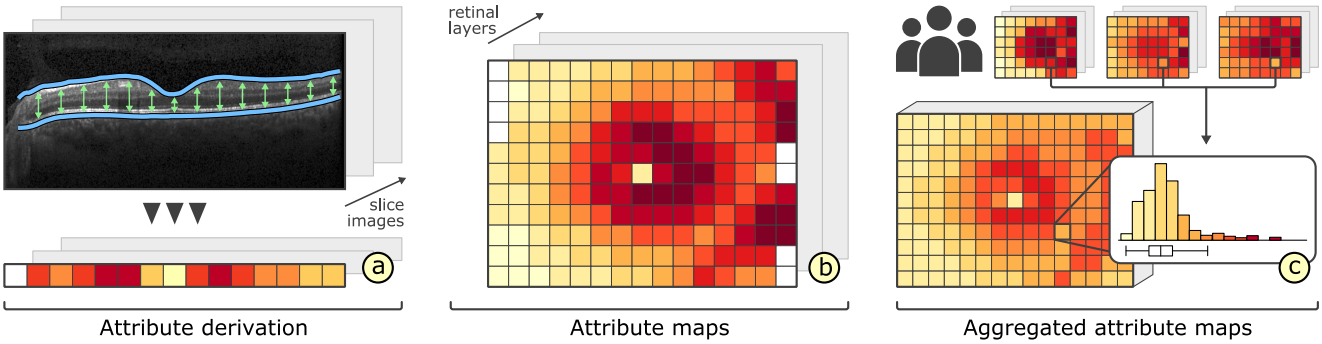

Fig. 2. Derivation of layer attributes. An attribute is computed by analyzing the extracted retinal layers in each acquired image slice of a dataset (a). One value is assigned to every pixel along the horizontal image axes, e.g., by measuring the vertical distance between the upper and the lower layer boundaries. The values are combined into 2D attribute maps for each extracted layer and each attribute definition (b). Aggregated attribute maps are compiled by applying summary statistics to all associated pixels in the individual maps from multiple datasets (c).

implement own prototypes to perform such tasks, since software libraries are provided with exclusive licenses and incomplete data specifications.

To develop visual analysis solutions for OCT data, it is essential to find a remedy for that issue. On this account, we adapt and extend previous work [35]. Particularly, we integrate a common data format and a library (UOCTE) that is capable of parsing data from the majority of current devices, e.g., Nidek, Eyetec, Topcon, and Heidelberg Engineering (DR_1). Based on the UOCTE library, we map the parsed data into one common domain. The result is independent from constrained manufacturer-provided functionality and it opens up new possibilities for data unification.

To structure the data, we utilize a common data modeling language (UOCTML), which accompanies the library (DR_2). UOCTML consists of an easily amendable XML file and a set of binary files for fundus, tomogram, and layers. The resulting data format promotes data exchange. Moreover, we are able to enrich the data with derived information and other medical records. To this end, we provide an associated interface with dedicated processing capabilities. It allows either to retrieve pre-segmented layer data or to apply basic layer segmentation methods directly (e.g., [23]). In addition, it enables extraction of OCT metadata and computation of several layer attributes.

Together, the UOCTE library, the UOCTML data format, and the interface represent initial steps towards the development of common data standards in the domain of OCT data. The software and associated specifications are freely available [36]. Further technical details regarding our efforts to unify distinct OCT data sources are described in [35].

5.2 Derivation of Layer Attributes

To facilitate the analysis of OCT data, we incorporate a set of derived attributes (DR_3). This is to inject meaningful information into the data that can help to characterize the condition of the retina. It allows us to condense complex OCT data down to information that is manageable and relevant. Moreover, the derived attributes capture even subtle and localized retinal changes. This way, they represent an effective starting point for the subsequent visual data analysis (cf. Sect. 6).

The attribute derivation comprises two steps that are carried out for each extracted layer. First, all points that define a layer's shape are enriched with derived attribute values. Figure 2 illustrates this process. This is to obtain attribute maps that characterize different layer properties, e.g., thickness maps. Second, for each attribute, a ranking of the layers is computed. A layer's rank is determined by analyzing the distribution of attribute values and their spatial locations in the attribute maps. The exact way how a ranking is computed can be controlled via different parameters. That is, the ranks are either defined by the total ratio of attribute values that are considered abnormal in a map or by the amount and size of connected abnormal regions. In addition, weights can be assigned to regard certain areas on a layer with abnormal characteristics more important than others. For instance, a targeted investigation may adapt the ranking to favor localized changes only in selected sectors of the ETDRS grid. This helps users to focus on layers with specific patterns.

In general, a single attribute alone will not suffice to capture all abnormal conditions of the retina. Therefore, we consider a collection of layer properties to target symptoms of different ocular diseases. In previous works mainly the thickness of the retinal layers has been studied to distinguish abnormal eyes from he-

althy eyes (e.g., [6, 9]). Based on discussion with domain experts, we additionally incorporate several other properties. Examples are the curvature of the layers' shapes or the homogeneity of OCT values enclosed by layer boundaries. This may help to detect localized deformations, e.g., drusen induced in an early stage of age-related macular degeneration, and variations in reflectivity, e.g., small macular holes or fluid deposits caused by diabetic retinopathy, respectively. Deriving corresponding attribute maps enables a more sophisticated investigation of the different layer properties.

Based on the individual attribute maps, we also support the computation of reference data (Fig. 2c). The user can select any group of OCT datasets and compute aggregated attribute maps for single or multiple attributes per layer. As the datasets may cover different retinal areas, the individual attribute maps are projected into a common spatial frame of reference, e.g., using the center of the fovea and of the optic disk as reference points. Each point of an aggregated map then stores summary statistics of the individual attribute maps, e.g., mean, range, standard deviation, and histograms. This provides a compact representation of multiple OCT datasets. Moreover, it facilitates overview and comparison, while being spatially more precise than analysis approaches based on global data reduction according to ETDRS grids (cf. Sect. 2). If necessary, such currently common abstractions of attribute values are easily derived from individual or aggregated attribute maps.

On top of the common data basis and derived layer attributes, we develop a visual analysis tool with augmented visualization techniques for the attributed OCT data (DR_4), which will be specified in the next section.

6 Visualize, Emphasize, Select & Compare Data

We aim at supporting users in visually analyzing OCT data and related information. For this purpose, we design a flexible visualization tool based on multiple coordinated views. Figure 3 shows an overview of the user interface. Our tool supports: (i) visualizing the data, (ii) emphasizing details, (iii) selecting subsets, and (iv) comparing multiple aspects.

6.1 Visualizing Data

In order to facilitate a comprehensive analysis of attributed OCT data, we visualize different types of information. Our solution shows raw data together with extracted layers, considers derived information, takes the quality of the data into account, and facilitates the exploration of relationships ($VR_1 + VR_2$). To this end, we support four types of views: (i) a 2D top-down view, (ii) a 3D view, (iii) a 2D cross-sectional view, and (iv) a view for related information.

The 2D top-down view provides an overview of derived attribute maps with regard to the interior surface of the eye (Fig. 3a). The OCT acquisition area is visualized on top of a fundus image. Each acquired image slice is represented as a line. All extracted retinal layers are shown as thumbnails on the side, ordered according to the computed rankings. Optionally, the thumbnails are enlarged and superimposed over the fundus image. Derived attribute maps are color-coded using suitable and adjustable palettes [22]. The opacity of the overlay can be adjusted using a slider, e.g., to help to relate attribute values in the maps to noticeable structures in the subjacent fundus image. If required, colored ETDRS grids are shown in addition to the maps. This design extends existing displays, in that it allows to view attributes for all layers in one image without having to flip through them manually. Hence, layers with abnormal characteristics can be easily discovered.

The 3D view shows the tomogram together with the extracted layers at a glance (Fig. 3b). The raw data are visualized via direct volume rendering and the layers are displayed as surfaces. Blending both 3D presentations allows to relate the tomogram to the layers. On demand, the layer surfaces are color-coded based on derived attributes. This illustrates interrelations between attribute values and the layer shapes. For spatial reference, a fundus image can be vertically moved through the display. Showing the data in 3D allows for a faithful representation of internal retinal structures. This way, regions of interest can be precisely localized.

The 2D cross-sectional view supports the investigation of details and the comparison of several layers at once (Fig. 3c). The acquired 2D image slices are depicted individually. The extracted layers are displayed as superimposed lines along the horizontal image axes. This allows to identify the exact layer profiles, to visually relate them, and to check for segmentation errors. A detail chart shows plots of derived attributes of a single layer or of multiple layers. The chart is positioned below the image slices and aligned horizontally to maintain the spatial context. Layers and plots are associated with unique colors. Visualizing the layer profiles and the attribute plots together facilitates a more precise analysis and direct comparison in addition to the color-coded visual representations in the other views.

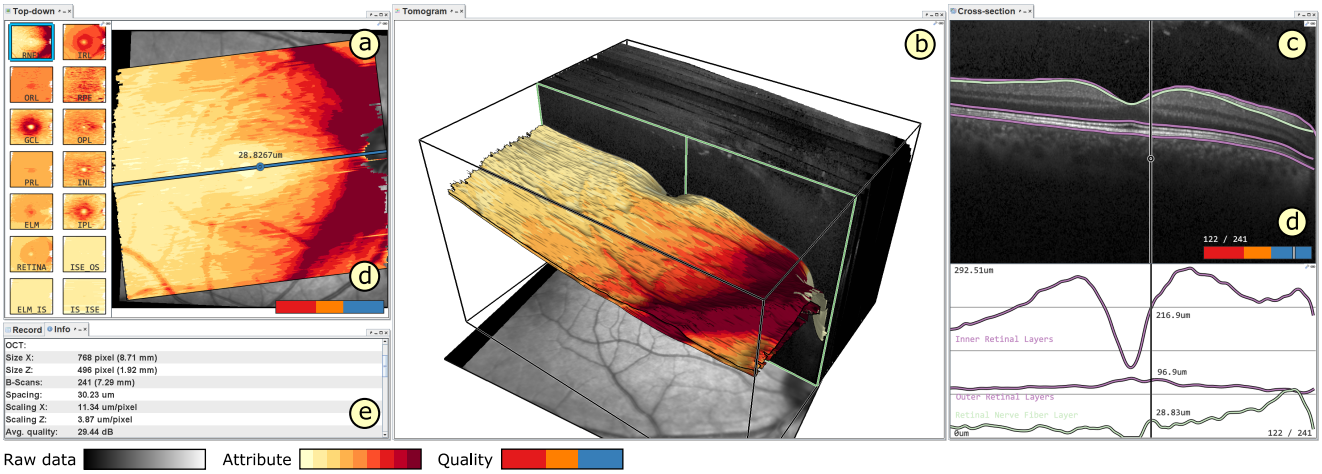

Fig. 3. Overview of our prototypical visual analysis tool. The user interface allows to add and arrange multiple linked views for visualizing different aspects of OCT data. Depicted are (a) a top-down view of the fundus overlayed with a derived attribute map, (b) a 3D view showing a volume visualization together with retinal layers as surfaces, (c) a cross-sectional view with extracted layers and a detail chart, and (e) a view for supplementary information. The signal strength of image slices is color-coded and shown together with associated legends (d).

Data quality is an important characteristic of OCT data [25, 30]. It has to be considered to prevent wrong conclusions from the data analysis. Therefore, in the first three views, missing values are either mapped to a special highlighting color to bring them to the users attention or to a background color to focus on certain parts of the data instead. Moreover, quality measures, e.g., the signal strength for 2D image slices, and associated legends are displayed in each view (Fig. 3d). Indicating the data quality helps to differentiate between artifacts and actual retinal changes, and thus aids the assessment of findings.

The information view displays general properties of datasets, logs about selected values, or other patient-related records (Fig. 3e). Depending on the type of information, different basic visualizations are available, e.g., tabular presentations or document viewers. In case multiple datasets are loaded, the view can show respective listings and help to assign datasets to the other views. This allows users to directly check the additional information together with the different perspectives of the shown OCT data, without having to rely on external software tools.

6.2 Emphasizing Data

Showing important information in the context of entire datasets is essential for visually analyzing complex OCT data [24]. We support users in comprehending the data by emphasizing spatial relationships and characteristic data values (VR_3). For this purpose, we provide methods for both spatial and data-oriented accentuation. Figure 4 illustrates how these methods can be applied.

Spatial emphasis conveys the spatial properties of the visualized data. This is crucial in the 3D view (Fig. 4a). We consider two illumination methods: a local technique based on a directional lighting model and a global approach based on ambient aperture lighting [29]. Directional lighting illustrates the general shape of the volumetric data and enhances the perception of small-scale spatial structures. Ambient aperture lighting highlights details and relationships between neighboring parts on the layer surfaces. Stylization further emphasizes certain spatial properties. On the one hand, enhancing edges makes it easier to distinguish spatial features of the tomogram and the layers. On the other hand, customized toon-shading generates a continuous abstraction of the layers that also reinforces the perception of depth [4]. Optionally, stereoscopic rendering can be activated to further facilitate 3D spatial perception.

Data-oriented emphasis highlights values of interest and steers the user's attention. For this purpose, we utilize three visual variables: color, transparency, and blur [21]. In the 2D and 3D views, visual prominence is controlled via an interactive transfer function editor. The editor modifies the visual encoding to either strengthen or attenuate the influence of values in the rendered images. For instance, invalid values may be filtered out by lowering their opacity. Other value ranges can be assigned to special color palettes to compare them in the different views. The views are linked with the editor and automatically update according to user input.

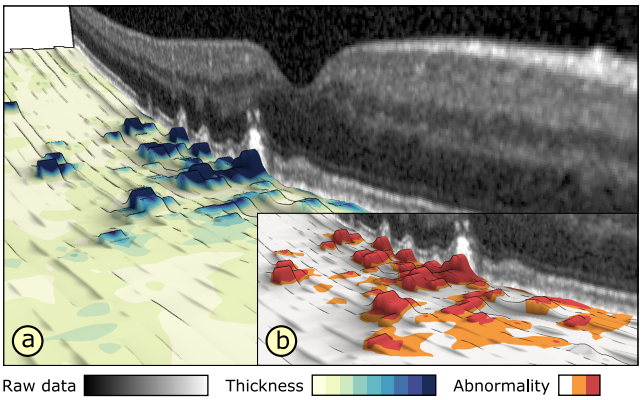

Fig. 4. Selecting and emphasizing data. The 3D view shows a selected layer, colored by its thickness (thin: green, thick: blue). Illumination and enhanced edges facilitate the spatial perception of the layer's shape (a + b). Abnormal thickness according to predefined thresholds is emphasized via spatial and data-driven selections (b). The small scattered elevations (orange, red) indicate the presence of drusen, a sign for age-related macular degeneration.

Figure 4b shows an example of modified colors for identifying abnormal attribute values. To further steer the user's attention, data-oriented emphasis is generated via customized depth-of-field rendering [26]. Regions with values of interest are depicted sharply, whereas their surroundings are blurred in the visualization. This helps to focus on details and to maintain the context at once.

Spatial emphasis and data-oriented emphasis can also be combined. This is valuable for relating certain data values to spatial properties. For example, in the 3D view, abnormal attribute values are highlighted using color. Applying enhanced edges illustrates their relationship to the shape of the layers, while still being able to precisely read off different color shades. In addition, toon-shading or depth-of-field rendering can be activated to support the identification of affected regions.

6.3 Selecting Data

To enable the exploration of large OCT datasets, the data have to be reduced to relevant subsets. We support this via coordinated selection techniques (VR_3). Subsets are interactively defined both spatially and data-driven. Figure 4 exemplifies the application of both techniques.

Spatial selections enable users to specify regions of interest. We integrate various selection methods based on points and geometric shapes. Individual points can be selected in all views to show their assigned values via tooltips. In the 3D view, tomogram and layer selections are realized via interactive clipping geometry, including planes, spheres, or layer surfaces. For example, clipping the tomogram via adjustable planes helps to relate selected parts to the layers (Fig. 4a). In the 2D views, polygon selection allows users to interactively set multiple corners to define spatial regions of interest. Users can choose to apply such selections to single image slices and layers, or to groups of them. This way, inspecting the same regions in different parts of the data is possible. All spatial selections can be expanded or reduced using binary operations. The provided selection methods aid the specification of precise boundaries of spatial regions, and hence are an effective way to reduce the data directly via their visual representation.

Data-driven selections permit users to specify value ranges of interest. For raw OCT data, the transfer function editor facilitates selecting one or multiple value ranges. To support such selections, a histogram is shown for reference. For derived attributes, users can choose which attributes are to be mapped onto the layer representations (Fig. 4b). This helps to focus on those data characteristics and to relate them to their spatial context. In addition, the detail chart in the 2D cross-sectional view enables selecting value ranges by brushing parts of the attribute plots. Data-driven selections allow to capture all regions with specific data characteristics across entire datasets, which would be hard to dissect via direct spatial selections in the views.

Specified selections can be applied in two ways: locally, i.e, solely in one view, or globally, i.e., by automatically propagating them to interlinked views. Moreover, selections may be applied in combination with the emphasizing methods to adapt the visual representations. This allows to show subsets either exclusively or highlighted in context of other data. For example, global selections support linking and brushing. Selecting a point in one view shows respective cursors in all other views. To browse through the data, the cursor in the top-down view is moved. The 3D view and cross-sectional view are updated accordingly and continuously display matched image slices and clippings of the tomogram. This allows to quickly access and relate different parts of the data.

6.4 Comparing Data

Subtle retinal changes can often only be revealed by relating two or more datasets to each other. Hence, besides displaying one dataset of one individual at a time, our tool also allows to visually compare multiple intraindividual datasets, e.g., from follow-up examinations, and interindividual datasets, e.g., from cohort studies (VR_4). We support this via a combination of superposition and

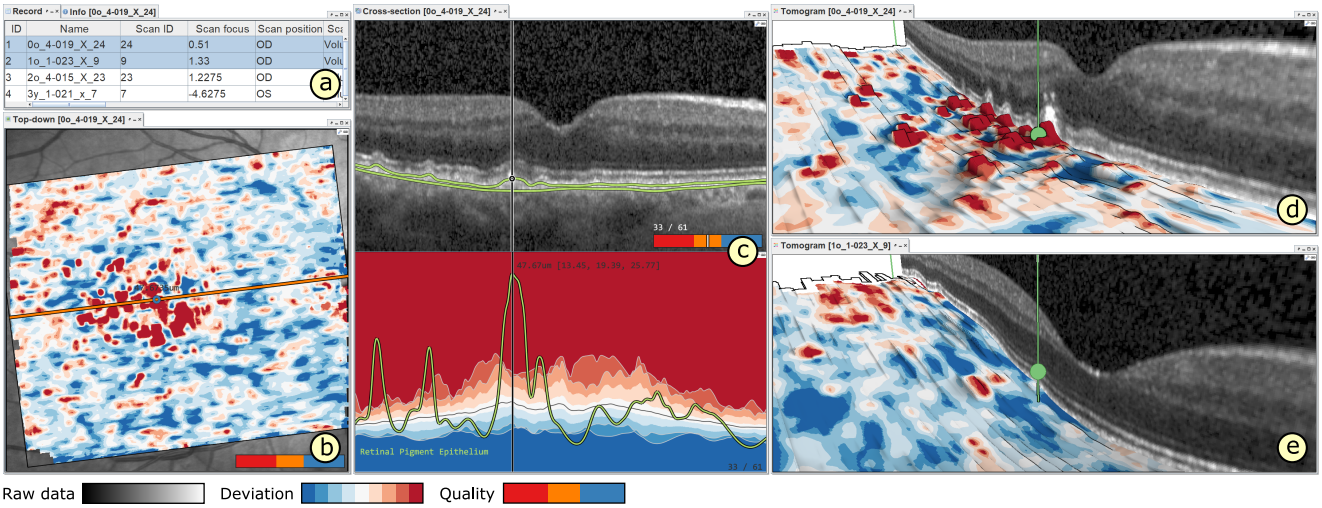

Fig. 5. Comparison of multiple datasets. Two datasets are selected in the information view (a). The first dataset is assigned to views (b, c, d) and the second dataset to view (e). Deviations of layer thickness from a confidence interval of reference data are color-coded using lighter colors for values close to the reference mean and darker colors for values outside the interval. The upper and the lower 3D views (e + d) are linked to show matched parts of each dataset.

explicit encoding of deviations, and juxtaposition of interlinked views (cf. [19]). Figure 5 shows an overview of the user interface for visual comparisons.

Encoding deviations enables comparing one dataset to reference data. This is possible by adapting the visual representation of extracted layers in the 2D views and 3D views (Fig. 5b + d). On demand, the coloring of the layers is switched to show derived attributes in relation to summary statistics stored in aggregated attribute maps (cf. Sect. 5.2). Different properties of the attribute maps can be chosen for the encoding. Examples are deviations to the mean or to a confidence interval of the reference data. The resulting deviation maps are encoded using diverging color palettes [22]. Optionally, properties of the reference data can be inspected on their own or in relation to other reference data.

The chart in the 2D cross-sectional view shows deviations for selected image slices in detail (Fig. 5c). Attribute profiles are depicted as superimposed line plots on top of the mean, the minimum, the maximum, and percentiles of the reference data. The chart's background is either colored according a confidence interval to match the encoding in the other views, or based on a histogram to show the distribution of the reference data.

Switching to this encoding allows to countercheck findings made while analyzing a dataset on its own. Moreover, subtle and localized changes can be easily detected and compared to raw data and extracted layers with high spatial specificity.

Juxtaposing views supports comparing several individual datasets simultaneously (Fig. 5d + e). The user interface allows to dynamically add and freely arrange instances of the four types of views. Using the information view, listed datasets can be selected and assigned to any other view instance simply via drag and drop (Fig. 5a). Those view instances then automatically update and show the respective OCT data directly. This allows to quickly switch between datasets. At the same time, specified selections and emphases are maintained to facilitate comparison of data aspects. To compare multiple datasets at once, one view instance is created per dataset. Juxtaposing and linking the view instances ensures that matching parts of the data are shown during navigation. All navigation is smoothly animated to prevent sudden changes in the rendered images. For example, different parts of the data can be explored in the 3D views via an interactive virtual camera and in the 2D views via zooming and panning. Relating the shown data back to the selected datasets is supported via special highlighting colors.

Applying such a view layout helps to analyze several data aspects in multiple datasets. Based on the common data basis this is even possible for datasets acquired via different OCT devices. This provides a distinct advantage compared to existing software tools that are based on fixed layouts, and thus only allow to visualize one aspect of one dataset at a time.

Figure 5 shows an example of comparing datasets of two patients to data of a control group. In the 2D top-down view and the 3D views the layers are colored by setting the patients' attribute values in contrast to the 95% interval of the control data. Light colors mark areas on the layers with thickness values close

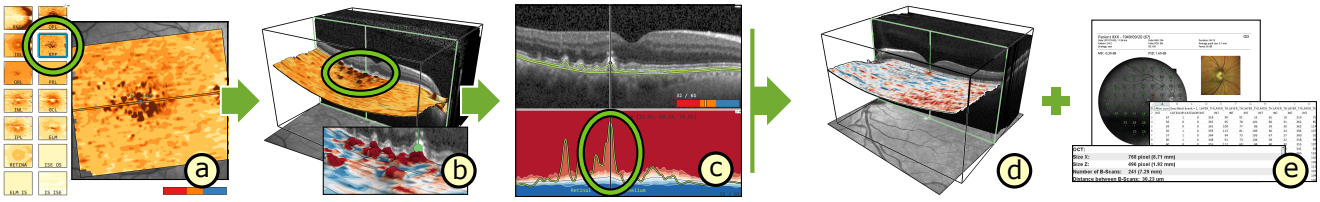

Fig. 6. Exemplary analysis workflow. An OCT dataset is gradually reduced to relevant information by selecting a layer in the top-down view (a), defining a region of interest in the 3D view (b), and inspecting details in the cross-sectional view (c). The obtained findings are then compared to further datasets (d) or to results of other examination methods (e).

to the reference mean, whereas dark colors indicate thinning or thickening outside the reference interval. In addition, one 3D view is added for each dataset. The upper 3D view is adjusted to show a region of interest. These view settings are dragged onto the second 3D view below. The second view automatically adapts according to the applied changes and shows the same region and encoding. This way, abnormal retinal changes can be easily detected in each dataset and subsequently compared to each other via the juxtaposed views.

6.5 Analysis Example

Our prototypical visualization tool can be applied in various ways. Figure 6 illustrates an exemplary analysis workflow. First, the overview of derived attribute maps in the top-down view helps to identify and select a retinal layer with abnormal characteristics (Fig. 6a). Enlarging the attribute map over the fundus image reveals centralized abnormal changes in the selected layer. Second, visualizing the layer in the 3D view allows to compare the attribute values to the layer's shape and to the volume rendering of the raw tomogram (Fig. 6b). This way, a region of interest can be localized and selected. Third, to analyze the region in detail, individual image slices and respective attribute plots are shown in the cross-sectional view for the specified region (Fig. 6c). Comparing the region to reference data is possible by loading an aggregated attribute map. Deviations of attribute values are emphasized by switching the color-coding and applying further stylization methods. Finally, the findings can be directly related to additional OCT datasets (Fig. 6d), e.g., a follow-up dataset, or to results of other examination methods (Fig. 6e). Applying such an analysis procedure promotes an informed interactive reduction of complex OCT data to clinical relevant information.

7 Application

In this use case, we applied our solution in cooperation with domain experts to study if retinal changes in pediatric patients suffering from type 1 diabetes mellitus (T1DM) can be visualized in comparison with healthy control subjects of the same age. Interestingly, none of the patients showed signs of diabetic retinopathy in results of other examination methods. In fact, the principal goal of this study was to identify changes of the retina that occur in a very early stage of a primary disease, e.g., diabetes mellitus. These changes are precursors of secondary complications that may lead to severe structural and functional defects. Secondary complications, e.g., diabetic retinopathy, are often only diagnosed in an advanced state once symptoms are obvious. However, the high sensitivity of OCT and the visual analysis of OCT data support detecting subtle and localized changes, and hence may contribute to an early diagnosis and immediate intervention.

The study data were acquired via OCT examination of two groups of subjects. The first group consists of 19 children with T1DM (⌀ 14.2 years of age, ⌀ 5.25 years duration of T1DM) and the second group of 30 healthy controls with matched sex and age (⌀ 14.3 years of age). For each subject, one volumetric OCT dataset of the macula was selected for further investigation (49 datasets in total). In a pre-process, aggregated attribute maps were computed for both groups. Individual attribute maps for all layers in the datasets were derived on the fly during visualization.

We jointly applied our tool to analyze the study data. In addition, a currently common analysis procedure based on statistical evaluation of ETDRS grids was performed (cf. Sect.2). Figure 7 summarizes a part of the obtained results.

Relating Patients to Controls: We started by visually comparing the aggregated attribute map of the patient group to the map of the control group (Fig. 7a). Deviations of the mean values in both maps were color-coded. The resulting visualization demonstrated that patients exhibit thinning primarily in pericentral ETDRS sectors around the fovea for several retinal layers, e.g., retinal nerve fiber layer, ganglion cell layer, and inner plexiform layer. These first insights are in accordance with the statistical analysis results and findings of previous

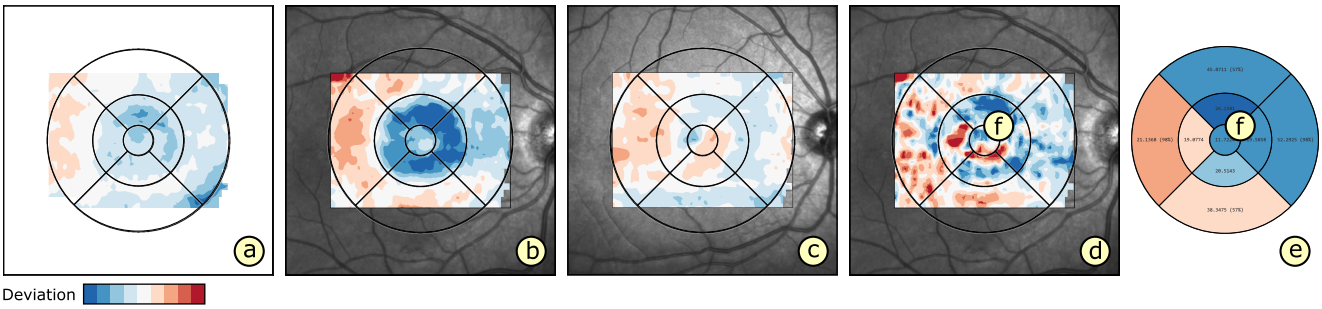

Fig. 7. Selected results from analyzing data of a clinical study in our use case. The layer thickness of patients with T1DM is compared to the 95% confidence interval of a healthy control group. The deviation maps show thinning (blue) and thickening (red) of the overall retinal thickness for the mean of all patients (a) and for two individual patients (b + c). Borders of an ETDRS grid are superimposed for spatial reference. The first map reveals pericentral (middle ETDRS ring) thinning across all patients (a). This is reflected by one of the patients (b), whereas the other patient exhibits slight thickening in the same area (c). Comparing a deviation map (d) to an ETDRS grid (e) shows that local pericentral thickening (f) of the retinal nerve fiber layer can be accurately captured with the map but not with the grid due to the applied data reduction.

work [8]. The experts stated that our approach eases the detection of such patterns and that it provides more spatial detail. Hence, hypotheses can be generated quickly without having to rely on external software.

Beyond group versus group analyses, also individual patients were compared to the reference data of the control group. This helped to explain the visualization of aggregated data and the results of the statistical evaluation. Apart from common patterns, different thickness patterns between patients were also identified. Figure 7b illustrates the data of one selected patient. The visualization clearly shows pericentral areas with reduced layer thickness. This confirmed prior assumptions and is in line with the group versus group analysis. In fact, by consulting related clinical information, the patient could be assigned to a subgroup of severe cases (long duration of T1DM + high blood sugar values). Observing the actual patterns of spatial changes and relating them to other aspects in the different views was new to the experts. For instance, some patients showed asymmetric patterns, e.g., temporal thickening and nasal thinning, in the peripheral ring of the ETDRS grids. Moreover, the experts discovered cases with less thinning or even marginal local thickening in pericentral areas (Fig. 7c). Most of these patients were subsequently categorized as mild cases (short duration of T1DM + low blood sugar values). This implies that even in mild cases, noticeable patterns can be detected with our tool. Thus, our visual analysis approach is effective in visualizing early retinal changes in pediatric patients with T1DM and no diabetic retinopathy.

Data Screening: The attribute maps allow to capture more information compared to ETDRS grids. This supports the data analysis in several ways. On the one hand, the experts can consider local variations during retinal assessment. Such information is often lost when looking at ETDRS diagrams alone (Fig. 7d + e). On the other hand, errors in the data can be detected easily. For example, at first the experts had identified local variations in attribute values for some datasets. However, these changes could later be traced back to segmentation errors. Visualizing the data quality of respective image slices and inspecting the layer boundaries for the affected areas helped the experts to come to this conclusion. Accordingly, an additional data screening pass was conducted with our tool. Some datasets were replaced by substitutes and others were marked for correction of segmentation errors. This way, only datasets of sufficient quality were included in the study.

The described results illustrate how our approach can be applied to gain insights into OCT data. Following, we outline how we designed and tested our solution together with domain experts.

8 User Feedback

Our solution is the result of a participatory design process starting from prior work [34] and [35]. We cooperated with a group of domain experts, including ophthalmic research scientists and ophthalmologists who deal with the treatment of retinal diseases. Throughout the development, we had close contact with primarily two experts. We jointly identified challenges and specified respective requirements (cf. Sect. 4). Their informal feedback helped us to design suitable visualizations and associated interaction techniques. While some design decisions were driven by the addressed data and task, e.g., the common data format and derivation of attributes, others were inspired by the domain experts, e.g., the comparison of datasets to reference data. The cooperation was of mutual benefit. We could build upon the

experts domain expertise and in turn, they benefited from our solution as it provided them with new insights into the data of their studies (cf. Sect. 7).

To ensure maximal practical relevance of the achieved results, we assessed our solution in repeated demonstration and feedback sessions together with the experts. The sessions were run using a pair analytics approach [2]. They were scheduled after each major development cycle and held at least once a month to review new functionality. One session typically lasted between one and two hours depending on the complexity of the added methods and associated analysis tasks. Mainly one visualization expert and at least one or two medical experts participated. The visualization expert played the role of the driver of the visual analysis tool, whereas the medical experts played the role of the navigator based on their contextual knowledge in the application domain. The data and analytical tasks were consistent between sessions and correspond to our use case. Selecting the use case, i.e., currently relevant tasks and familiar datasets, to test our solutions created a naturalistic setting for observations and reasoning. The tasks involved both free exploration, e.g., discovering abnormal characteristics in patients, and targeted investigations, e.g., retrieving values from specific deviation maps in group versus group comparison. Session protocols were recorded and exchanged after each session. In addition to the results outlined in the previous section, we obtained feedback regarding the general design and functionality provided by our tool.

During the discussions, the experts stated, that they liked the visual analysis tool because it allowed them to explore and relate different aspects of the data. They appreciated the consideration of established display concepts, e.g., the top-down view and the cross-sectional view. At the same time, the integration of our extensions was pointed out as meaningful, e.g., the overview of all extracted layers or the view for supplementary information. The experts also reassured us that the provided emphasis and selection methods are indeed helpful for inspecting different subsets in detail.

In earlier tests with initial prototypes of our tool, they had mentioned that the provided controls required some time to get accustomed with. Based on this feedback, we selected several interface components for a revision, including the controls of the virtual camera in the 3D view and control panels with associated display options. To come up with alternative solutions, we referred to available design guidelines (e.g., [15]) and prototyped new interaction concepts. For example, with respect to the 3D camera, we devised a new control mode that is solely based on mouse input, whereas before mouse and keyboard input was required. In addition, smooth animated transitions between camera movements were added to help users maintain their mental model during navigation. Regarding the interface, indirections were minimized by using direct manipulation where possible and by showing control panels with advanced settings only on demand. The reworked design was presented and discussed in subsequent feedback sessions together with the experts and again further refined. This iterative process improved the user experience substantially.

As a major advantage, the experts identified the ability to compare multiple and possibly differing datasets. The flexible interface and the interlinked views helped them to quickly switch between datasets and to show related information when necessary. For the analysis of larger studies, they considered the visualization of aggregated attribute maps to be particular useful. Utilizing these maps as reference data to compare individual datasets to groups of datasets helped them to detect even subtle and localized changes. In this regard, they approved to have both overviews, e.g., thumbnails of deviation maps in the top-down view, and detail views, e.g., the detail chart showing confidence intervals and histograms for image slices, at their disposal. Overall, they concluded that reducing the manual analysis effort and being able to obtain results with higher accuracy compared to the current analysis procedure are great benefits. In fact, for the first time, they were able to perform such analyses for volumetric macular OCT datasets. This is an important step towards finding characteristic retinal changes that indicate early symptoms of certain diseases.

Applying pair analytics to test and reflect on the introduced enhancements has been most fruitful so far, as it combines the expertise of visualization experts and domain experts. Findings in the data could be directly explained and new views were added or adapted on the fly to investigate further details. Applying our tool in this way triggered discussions and sparked new ideas for further improvements, which we will continue to share with the ophthalmic community (e.g., [33]). Besides, the experts recently asked us if we could provide them with a dedicated standalone version of our tool, so they are able to conduct further tests and apply it in clinical practice on their own. Accordingly, our tool will be used as a basis for further extension, fine-tuning, and evaluation together with them.

9 Discussion and Conclusion

We presented an interactive visual approach for managing, analyzing, and presenting OCT data. A unified data basis incorporates data from various devices and

derived information. A visual analysis tool supports exploration and emphasis of different data aspects, and selections of relevant subsets in interlinked views. Multiple datasets can be compared to each other and to reference data. Our approach constitutes a systematic enhancement of existing work, and hence can be a useful aid for retinal assessment using OCT.

Diagnostic Support: From an ophthalmic perspective, visual analysis of retinal OCT data may be utilized in various ways. With regard to clinical practice, it contributes in confirming retinal changes in relation to other clinical information and in getting a more complete idea of the retinal condition of individual patients. Therefore, the actual diagnosis and treatment decisions are often made on an individual basis only after detailed clinical and systemic investigation in addition to OCT analysis. With regard to ophthalmic research, visual analysis eases the evaluation of cohort studies and provides results with higher spatial specificity. This may lead to new insights into how certain pathologies affect the structures of the retina. The goal is to identify meaningful characteristics that can later be used to define biomarkers. In this regard, experimental and prospective studies, as presented in our use case, play an inherent role of ophthalmic research. We highly recommend additional prospective longitudinal studies to observe the structural changes over a period of time and to relate these changes with the functional aspects of the patients. To support such investigations, both qualitative and quantitative analyses of OCT data have to be integrated. Hence, we plan to extent our approach to support time-oriented data analysis and targeted statistical tests.

Data Support: Our data management is capable of parsing and converting data from different devices. By making the software sources freely available, we ensure its dissemination to an interested audience. This is a first step towards developing device-independent data standards. Although it remains difficult to cover all possible data sources, we will continue our efforts to support file formats of major manufacturers and retrieve respective metadata. In addition, we plan to directly relate the data to further information for characterizing the retina. This includes results from other examination methods, e.g., angiography or microperimetry, and diagnosis-related annotations. For this purpose, the common data basis has to be extended to adequately register, store, and exchange such information. Regarding the extraction of retinal layers, our data interface supports two methods. On the one hand, we retrieve pre-segmented layer information from proprietary data files of the OCT device manufacturers. On the other hand, if such information is not available, we provide basic segmentation methods [23] or use free software (e.g., [27]). Yet, this does not emulate the functionality of commercial software to its full extent. More work is required to integrate state-of-the-art segmentation algorithms (e.g., [13]). Directly incorporating advanced methods into our tool and disclosing related parameters, will help to reduce deviations between measurements and facilitate the comparison of analysis results from different datasets. In this regard, it remains to be studied to what extent existing algorithms can be adapted to address manufacturer-related differences in the data, e.g., varying numerical precision or noise characteristics.

Analytic Support: We aid the visual analysis of OCT data via various computational methods in our tool. This includes the derivation of layer attributes, the ranking of the layers, and the automated alignment of interlinked views. We plan to enhance our approach based on further feedback from domain experts. One particular request was to extend the support for analyzing multiple datasets. Interesting patterns could be automatically detected and subsequently suggested to the user. For example, similarly to the computation of layer rankings, the experts want to be able to search for matching subsets across datasets. One possible approach would be to extract and compare features based on attribute maps and reference data. An interesting open question is how we can find meaningful feature definitions that address specific analysis tasks, e.g., the identification of certain symptoms. This requires assistance in evaluating how well a feature captures certain characteristics and how the feature extraction process can be steered to obtain robust results.

Visual Support: The described examples demonstrate that our approach is suitable for analyzing multiple datasets at once. Visual comparison is supported either via explicit encoding of deviations to reference data or by assigning different datasets to juxtaposed views. However, adding multiple view instances only makes sense for up to two or three datasets at a time. Comparing numerous datasets by switching between multiple visualizations may not be the best solution. Hence, we plan to extend our tool to provide dedicated overview visualizations. An effective design would allow to directly compare the data of an entire study. Cognitive constraints and screen space limitations will be challenging factors to deal with. In a first prototype, we tested a small multiple design, which shows synchronized top-down views for several datasets in one image. This can be a feasible approach for tens of datasets. In the future, we will investigate alternative encodings that are scalable enough to handle even more datasets.

User Support: We ascertained the general utility of our solutions in first tests with domain experts (two being authors of this paper). To improve our design, we plan to integrate guidance for different diagnostic tasks. In this context, specifications of dedicated workflows and further evaluations of our tool will become necessary.

Acknowledgements The authors wish to thank Heidelberg Engineering GmbH for providing OCT hardware, and respective software interfaces and analysis software.

References

1. Aaker, G.D., Gracia, L., Myung, J.S., Borcherding, V., Banfelder, J.R., D'Amico, D.J., Kiss, S.: Three-dimensional reconstruction and analysis of vitreomacular traction: Quantification of cyst volume and vitreoretinal interface area. Archives of Ophthalmology **129**(6), 805–820 (2011). DOI 10.1001/archophthalmol.2011.123
2. Arias-Hernandez, R., Kaastra, L.T., Green, T.M., Fisher, B.: Pair analytics: Capturing reasoning processes in collaborative visual analytics. In: Proceedings of the Hawaii International Conference on System Sciences, pp. 1–10. IEEE Computer Society, Washington, DC, USA (2011). DOI 10.1109/HICSS.2011.339
3. Baghaie, A., Yu, Z., D'Souza, R.M.: State-of-the-art in retinal optical coherence tomography image analysis. Quantitative imaging in medicine and surgery **5**(4), 603617 (2015). DOI 10.3978/j.issn.2223-4292.2015.07.02
4. Barla, P., Thollot, J., Markosian, L.: X-toon: An extended toon shader. In: D. DeCarlo, L. Markosian (eds.) Proceedings of the International Symposium on Non-photorealistic Animation and Rendering, pp. 127–132. ACM, Annecy, France (2006). DOI 10.1145/1124728.1124749
5. Berufsverband der Augenärzte Deutschlands e. V., Deutsche Ophthalmologische Gesellschaft, Retinologische Gesellschaft e. V.: Quality assurance of optical coherence tomography for diagnostics of the fundus: Positional statement of the BVA, DOG and RG. Der Ophthalmologe **114**(7), 617–624 (2017). DOI 10.1007/s00347-017-0508-9
6. Chen, Q., Huang, S., Ma, Q., Lin, H., Pan, M., Liu, X., Lu, F., Shen, M.: Ultra-high resolution profiles of macular intra-retinal layer thicknesses and associations with visual field defects in primary open angle glaucoma. Scientific Reports **7**, 41,100 (2017). DOI 10.1038/srep41100
7. Chen, Y., Li, J., Yan, Y., Shen, X.: Diabetic macular morphology changes may occur in the early stage of diabetes. BMC Ophthalmology **16**(12) (2016). DOI 10.1186/s12886-016-0186-4
8. De Clerck, E.E., Schouten, J.S., Berendschot, T.T., Kessels, A.G., Nuijts, R.M., Beckers, H.J., Schram, M.T., Stehouwer, C.D., Webers, C.A.: New ophthalmologic imaging techniques for detection and monitoring of neurodegenerative changes in diabetes: a systematic review. The Lancet Diabetes & Endocrinology **3**(8), 653–663 (2015). DOI 10.1016/S2213-8587(15)00136-9

9. van Dijk, H.W., Kok, P.H.B., Garvin, M., Sonka, M., DeVries, J.H., Michels, R.P.J., van Velthoven, M.E.J., Schlingemann, R.O., Verbraak, F.D., Abràmoff, M.D.: Selective loss of inner retinal layer thickness in type 1 diabetic patients with minimal diabetic retinopathy. Investigative Ophthalmology & Visual Science **50**(7), 3404 (2009). DOI 10.1167/iovs.08-3143
10. Drexler, W., Morgner, U., Ghanta, R.K., Kärtner, F.X., Schuman, J.S., Fujimoto, J.G.: Ultrahigh-resolution ophthalmic optical coherence tomography. Nature Medicine **7**(4), 502–507 (2001). DOI 10.1038/86589
11. Duncan, M.D., Bashkansky, M., Reintjes, J.: Subsurface defect detection in materials using optical coherence tomography. Optics Express **2**(13), 540–545 (1998). DOI 10.1364/OE.2.000540
12. Early Treatment Diabetic Retinopathy Study Research Group: Grading diabetic retinopathy from stereoscopic color fundus photographs – an extension of the modified airlie house classification: ETDRS report number 10. Ophthalmology **98**(5), 786 – 806 (1991). DOI 10.1016/S0161-6420(13)38012-9
13. Ehnes, A., Wenner, Y., Friedburg, C., Preising, M.N., Bowl, W., Sekundo, W., zu Bexten, E.M., Stieger, K., Lorenz, B.: Optical coherence tomography (OCT) device independent intraretinal layer segmentation. Translational Vision Science & Technology **3**(1) (2014). DOI 10.1167/tvst.3.1.1
14. El-Fayoumi, D., Badr Eldine, N.M., Esmael, A.F., Ghalwash, D., Soliman, H.M.: Retinal nerve fiber layer and ganglion cell complex thicknesses are reduced in children with type 1 diabetes with no evidence of vascular retinopathy. Investigative Ophthalmology & Visual Science **57**(13), 5355 (2016). DOI 10.1167/iovs.16-19988
15. Elmqvist, N., Vande Moere, A., Jetter, H.C., Cernea, D., Reiterer, H., Jankun-Kelly, T.J.: Fluid interaction for information visualization. Information Visualization **10**(4), 327–340 (2011). DOI 10.1177/1473871611413180
16. Garrido, M.G., Beck, S.C., Mühlfriedel, R., Julien, S., Schraermeyer, U., Seeliger, M.W.: Towards a quantitative OCT image analysis. PLOS ONE **9**(6), 1–10 (2014). DOI 10.1371/journal.pone.0100080
17. Garvin, M.K., Abramoff, M.D., Wu, X., Russell, S.R., Burns, T.L., Sonka, M.: Automated 3-D intraretinal layer segmentation of macular spectral-domain optical coherence tomography images. IEEE Transactions on Medical Imaging **28**(9), 1436–1447 (2009). DOI 10.1109/TMI.2009.2016958
18. Glaßer, S., Hoffmann, T., Boese, A., Voß, S., Kalinski, T., Skalej, M., Preim, B.: Virtual inflation of the cerebral artery wall for the integrated exploration of OCT and histology data. Computer Graphics Forum (2016). DOI 10.1111/cgf.12994
19. Gleicher, M., Albers, D., Walker, R., Jusufi, I., Hansen, C.D., Roberts, J.C.: Visual comparison for information visualization. Information Visualization **10**(4), 289–309 (2011). DOI 10.1177/1473871611416549
20. Glittenberg, C., Krebs, I., Falkner-Radler, C., Zeiler, F., Haas, P., Hagen, S., Binder, S.: Advantages of using a ray-traced, three-dimensional rendering system for spectral domain cirrus HD-OCT to visualize subtle structures of the vitreoretinal interface. Ophthalmic Surgery Lasers and Imaging **40**(2), 127–134 (2009). DOI 10.3928/15428877-20090301-08
21. Hall, K.W., Perin, C., Kusalik, P.G., Gutwin, C., Carpendale, S.: Formalizing emphasis in information visualization. Computer Graphics Forum **35**(3), 717–737 (2016). DOI 10.1111/cgf.12936
22. Harrower, M., Brewer, C.A.: Colorbrewer.org: An online tool for selecting colour schemes for maps. The Cartographic Journal **40**(1), 27–37 (2003). DOI 10.1179/000870403235002042
23. Kahl, S., Ritter, M., Rosenthal, P.: Automated assessment of the injury situation in patients with age-related macular degeneration (AMD). In: F.P. Leon, M. Heizmann (eds.) Proceedings of Forum Bildverarbeitung, pp. 179–190. KIT Scientific Publishing, Regensburg, Germany (2014). DOI 10.5445/KSP/1000043608
24. Keim, D.A., Mansmann, F., Schneidewind, J., Thomas, J., Ziegler, H.: Visual Analytics: Scope and Challenges, pp. 76–90. Springer, Berlin, Heidelberg (2008). DOI 10.1007/978-3-540-71080-6_6
25. Koleva-Georgieva, D.N.: Optical coherence tomography – segmentation performance and retinal thickness measurement errors. European Ophthalmic Review **6**(2), 78–82 (2012). DOI 10.17925/EOR.2012.06.02.78
26. Kosara, R., Miksch, S., Hauser, H.: Semantic depth of field. In: Proceedings of the IEEE Symposium on Information Visualization, pp. 97–104. IEEE Computer Society, San Diego, CA, USA (2001). DOI 10.1109/INFVIS.2001.963286
27. Mayer, M.A., Hornegger, J., Mardin, C.Y., Tornow, R.P.: Retinal nerve fiber layer segmentation on FD-OCT scans of normal subjects and glaucoma patients. Biomedical Optics Express **1**(5), 13581383 (2010). DOI 10.1364/BOE.1.001358
28. Moisseiev, E., Park, S., Yiu, G., Werner, J.S., Zawadzki, R.J.: The third dimension: Advantages of 3D-OCT in retina – unprecedented detail of perfusion and other structures. Retinal Physician **13**,

24–33 (2016)
29. Oat, C., Sander, P.V.: Ambient aperture lighting. In: Proceedings of the Symposium on Interactive 3D Graphics and Games, pp. 61–64. ACM, Seattle, WA, USA (2007). DOI 10.1145/1230100.1230111
30. Odell, D., Dubis, A.M., Lever, J.F., Stepien, K.E., Carroll, J.: Assessing errors inherent in OCT-derived macular thickness maps. Journal of Ophthalmology **2011** (2011). DOI 10.1155/2011/692574
31. Placet, V., Méteau, J., Froehly, L., Salut, R., Boubakar, M.L.: Investigation of the internal structure of hemp fibres using optical coherence tomography and focused ion beam transverse cutting. Journal of Materials Science **49**(24), 8317–8327 (2014). DOI 10.1007/s10853-014-8540-5
32. Probst, J., Koch, P., Hüttmann, G.: Real-time 3D rendering of optical coherence tomography volumetric data. In: P.E. Andersen, B.E. Bouma (eds.) Proceedings of SPIE Optical Coherence Tomography and Coherence Techniques IV, pp. 73,720Q – 73,731Q. SPIE, Munich, Germany (2009). DOI 10.1117/12.831785
33. Röhlig, M., Jünemann, A., Fischer, D.C., Prakasam, R.K., Stachs, O., Schumann, H.: Visual analysis of retinal OCT data. Klinische Monatsblätter für Augenheilkunde **234**(12), 1463–1471 (2017). DOI 10.1055/s-0043-121705
34. Röhlig, M., Rosenthal, P., Schmidt, C., Schumann, H., Stachs, O.: Visual analysis of optical coherence tomography data in ophthalmology. In: M. Sedlmair, C. Tominski (eds.) Proceedings of the EuroVis Workshop on Visual Analytics (EuroVA). The Eurographics Association, Barcelona, Spain (2017). DOI 10.2312/eurova.20171117
35. Rosenthal, P., Ritter, M., Kowerko, D., Heine, C.: OphthalVis – making data analytics of optical coherence tomography reproducible. In: K. Lawonn, M. Hlawitschka, P. Rosenthal (eds.) Proceedings of EuroVis Workshop on Reproducibility, Verification, and Validation in Visualization. The Eurographics Association, Groningen, Netherlands (2016). DOI 10.2312/eurorv3.20161109
36. Rosenthal, P., Ritter, M., Kowerko, D., Heine, C.: Unified OCT explorer. `http://bitbucket.org/uocte/` (2016)
37. Schindelin, J., Rueden, C.T., Hiner, M.C., Eliceiri, K.W.: The ImageJ ecosystem: An open platform for biomedical image analysis. Molecular Reproduction and Development **82**(7-8), 518–529 (2015). DOI 10.1002/mrd.22489
38. Schulze, J.P., Schulze-Döbold, C., Erginay, A., Tadayoni, R.: Visualization of three-dimensional ultrahigh resolution OCT in virtual reality. Studies in health technology and informatics **184**, 387–391 (2013). DOI 10.3233/978-1-61499-209-7-387
39. Sylwestrzak, M., Szlag, D., Szkulmowski, M., Targowski, P.: Real-time massively parallel processing of spectral optical coherence tomography data on graphics processing units. In: R.A. Leitgeb, B.E. Bouma (eds.) Proceedings of SPIE Optical Coherence Tomography and Coherence Techniques V, pp. 80,910V–80,917V. SPIE, Munich, Germany (2011). DOI 10.1117/12.889805
40. Wojtkowski, M., Srinivasan, V., Fujimoto, J.G., Ko, T., Schuman, J.S., Kowalczyk, A., Duker, J.S.: Three-dimensional retinal imaging with high-speed ultrahigh-resolution optical coherence tomography. Ophthalmology **112**(10), 1734 – 1746 (2005). DOI 10.1016/j.ophtha.2005.05.023
41. Yoshimura, N., Hangai, M.: OCT Atlas. Springer, Berlin, Germany (2014)